Eindhoven University of Technology

MASTER

Collision avoidance using multiple correlated 3D depth measurements

Hamermans, Ivo W.J.

Award date:
2011

Link to publication

Disclaimer
This document contains a student thesis (bachelor's or master's), as authored by a student at Eindhoven University of Technology. Student theses are made available in the TU/e repository upon obtaining the required degree. The grade received is not published on the document as presented in the repository. The required complexity or quality of research of student theses may vary by program, and the required minimum study period may vary in duration.

General rights
Copyright and moral rights for the publications made accessible in the public portal are retained by the authors and/or other copyright owners and it is a condition of accessing publications that users recognise and abide by the legal requirements associated with these rights.

- Users may download and print one copy of any publication from the public portal for the purpose of private study or research.
- You may not further distribute the material or use it for any profit-making activity or commercial gain

Collision Avoidance Using Multiple Correlated 3D Depth Measurements

I.W.J. Hamersma

CST 2011.034

Master's thesis

Committee: prof.dr.ir. M. Steinbuch (chairman)
prof.dr.ir P.P. Jonker
dr.ir. M.J.G. van de Molengraft (coach TU/e)
ir. J. Dries (coach Philips)
ir. M.J.H. den Hartog (coach Philips)
dr.ir. Y. Morvan (coach Philips)

Eindhoven University of Technology
Department of Mechanical Engineering
Control Systems Technology Group

Eindhoven, June, 2011

Collision Avoidance Using Multiple Correlated 3D Depth Measurements in Unknown Dynamic Robotic Environments

Graduation Report I.W.J. Hamersma CST2011.034

Ivo Hamersma, Marinus v.d. Molengraft, Maarten Steinbuch, Johan Dries, Mark d. Hartog, Yannick Morvan

Abstract—In this paper a new approach for collision avoidance in an unknown $3D$ dynamic robotic environment based on evaluation of depth image data is proposed. By merging multiple depth measurements with respect to the environment, a $3D$ free space model can be reconstructed wherein the intended movements of the robot can be validated. Collision avoidance is verified by projecting new positions of the robot in the reconstruction and search for any common areas with other present objects. To verify the volumetric voxel reconstruction, a simulation model is used that serves as ground truth. By comparing all voxels, a quantitative accuracy of the reconstruction is given. In this paper, a medical intervention room with a motorised C-arc is taken as an example for the robotic environment, where humans and the C-arc have the same working area. Experimental results show an average accuracy of 98.8% of free spaces and 91.1% of objects, where all collision tests give correct verdicts.

Index Terms—3D Sensor, Collision Avoidance, Robots, Safety, Unknown Dynamic Environment.

1 Introduction

During operation, robots or other motorised equipment are not desired to collide with humans or objects in order to prevent injuries or damage. In most current applications, the working area of a robot is completely separated from the working area of other robots or humans, which is not possible for all applications. For example, in many medical applications, motorised imaging equipment has the same working area as the doctors.

In this paper, we explore how to provide the system with information about the free moving areas by use of depth sensors. The depth information that is provided by these sensors is interpreted as free space between the sensor and the measured object.

To handle occlusions, which can occur if 2 or more objects are present in the scene, the information from multiple sensors need to be merged. By merging the provided depth information from each sensor into a volumetric model, it can be determined whether a volumetric element is occupied or free. The dimensions of the volumetric model are defined by the working area of the robot.

In heterogeneous environments it is often not desirable to attach sensors to the moving equipment itself because of hygiene or reduced area of reach. It also may be necessary to obtain information outside the field of view of sensors attached to the robot. Therefore it is chosen to attach the sensors to the surroundings such that they have an overview on the scene which makes that they can provide a static point of view on the scene.

For the moving equipment it is assumed that a $3D$ model is available. Knowing the current and future positions and orientations of the controlled equipment, together with its $3D$ model, it can be calculated whether or not a collision can be expected.

Because no a priori information about the sur-

- *I.W.J. Hamersma, M.J.G. v.d. Molengraft and M. Steinbuch are with the department of Mechanical Engineering at Eindhoven University of Technology, Eindhoven, The Netherlands. i.w.j.hamersma@student.tue.nl, m.j.g.v.d.molengraft@tue.nl, m.steinbuch@tue.nl .*
- *J. Dries, M.J.H. d. Hartog and Y. Morvan are with Philips Healthcare within the Business Unit Interventional Xray, Best, The Netherlands. johan.dries@philips.com, mark.den.hartog@philips.com, yannick.morvan@philips.com*

Manuscript not submitted yet.

roundings is taken into account, the proposed system is able to work under any conditions, number of cameras, number of objects and orientation of objects. In general, an increase in the number of cameras and/or a decrease in the number of objects is expected to give an improvement of performance, where performance is indicated by the reconstruction accuracy and safe collision avoidance.

To verify the concept of using multiple correlated depth sensors for collision avoidance, several simulations will be executed by use of the $3D$ content suite Blender [20]. The simulated model being used as ground truth, both the accuracy of the reconstruction and the collision avoidance algorithm can be verified. Using a $1:5$ scale model, a real world proof of concept is given.

2 Prior Work

This paper focusses on the design of a multiple-depth-sensor system that can detect free space around a moving machine in an unknown environment for the purpose of collision free movements.

In the past, several approaches for sensor-based collision avoidance have been discussed. The approach as presented in [1] uses a back projection of the model of the robot onto the images that are captured and tries to give a safety distance measure. This method only gives a qualitative result based on image pixels, whereas a quantitative measure is needed. In [2], correlation between cameras is used to reduce the effect of occlusions for an object tracking method. A simplified version of this method is used to improve the reconstructions in our method. Another approach is presented in [3], where motion sensors are attached to the humans to measure and predict their motions and use this knowledge to prevent collisions. Because it is not desired to attach any sensors to the objects, this method is not suitable for our implementation.

To make it possible to predict if planned movements are possible, a reconstruction of the environment is needed. The method as presented in [4] uses a database of object models to reconstruct them in a $3D$ environment, where [8] uses object similarity across multiple images to reconstruct the object. A disadvantage of both methods is that they only can handle a single object because these methods assume that all detected surfaces belong to one object. In [5]–[7], reconstruction methods are proposed that use a discrete volumetric representation of the scene, also known as voxels, to make it possible to use a quantitative measure. Where these methods reconstruct objects by use of colour images, the goal for this paper is to reconstruct the free spaces by use of depth images. This method is chosen because no object information such as colour or shape are needed for the reconstruction.

Optimising the placement of sensors to optimally view the full volume is a problem similar to the Art Gallery Problem [12], where the number of guards and their positioning needs to be optimised. [10] presents a solution to place the sensors such that all objects in the volume can be seen, which method is only suitable for fixed setups. In [11] a $2D$ method is presented to distribute sensors such that all volume can be seen by a single sensor, but this method does not to take occlusions into account and is therefore not suitable for our method.

The work as presented in this paper extends the work as presented in [9], in which a single Time-of-Flight camera was used for the surveillance of a small part of a robotic working area. In [9], it was only possible to move the robot safely in the direction perpendicular towards the camera, if no other objects obstruct the sight on the robot. By using multiple correlated $3D$ depth sensors, the concept as presented in this paper is able to generate a $3D$ free space reconstruction of the scene. By using the known and future positions of the moving equipment, collisions can be predicted and therefore avoided.

The contributions of this paper are:

- Creating a $3D$ free space model using the Depth Buffer Algorithm on depth images.
- Defining a method to verify sensor positioning.
- Validation of the concept using simulations and a scale model.

3 Free space reconstruction

This research focuses on a free space reconstruction that enables motorised equipment to asses information whether or not the intended movement is safe. For a collision avoidance system, it is desired that any collisions are avoided, but at the same time false stops must be avoided as well.

It is chosen to design a setup that reconstructs all free space in the working area of the equipment, such that the equipment can safely operate in the free space.

For this research, the working area of a ceiling suspended C-arc is taken into account. A C-arc is a movable imaging device with an X-ray source

and detector, which is used for taking images during minimal invasive surgery. The area of interest, which is defined by the area of reach of the C-arc, is $4 \times 4 \times 2.5[m]$. To make the situation as realistic as possible, a C-arc, patient table, monitor ceiling suspension, operation light, patient, doctor, two nurses and three cabinets are placed in the simulated intervention room.

For the construction of this free space model it is chosen to discretise the volume into cubic voxels. Because it is searched for free space, all volumetric elements are initialized as occupied. By using the measurements, the occupancy of each voxel can be determined. To make the concept of this paper as general as possible, the only restriction for the sensor is that it can generate an image with depth information.

3.1 Depth Buffering

To be able to determine the occupancy of each of the voxels, a modified version of the depth buffer algorithm [21] is used. For each camera, the depth of each world point $d_{world} = \sqrt{X^2 + Y^2 + Z^2}$ is compared to the depth measured by the corresponding pixel $d_{pix(u,v)}$.

In the depth buffer algorithm it is verified whether or not a point can be directly seen from a camera point or that it is occluded. In our implementation the depth buffer algorithm is used to verify whether or not the representation of a voxel in the sensor is shorter or larger than the measured distance. If the measured distance is larger than the distance to the designated voxel, the voxel will be declared as a free F, where it is left as occupied O in other cases. To handle occlusions, once a voxel is declared as free F, it cannot be set as occluded O by other cameras.

3.2 Data Merging

To merge the free spaces in the volume, the data of each $3D$ sensor needs to be converted to the world model. For the sensor, a pinhole camera model [14] is used with the optical axis being collinear with the depth axis Z, as validated in [13].

To be able to combine the acquired depth information from all sensors, both intrinsic as extrinsic parameters are needed. The extrinsic parameters are the translation T and rotation R matrices that correlate the sensor position with respect to the world coordinate frame, where the intrinsic parameters such as the focal distance f and the principle

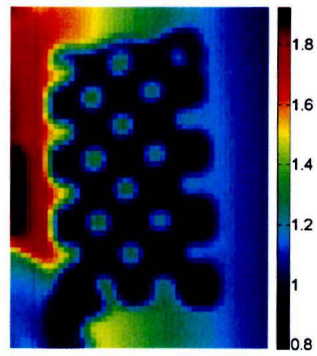

Fig. 1: Depth Image of transparent checkerboard obtained by a Time of Flight camera

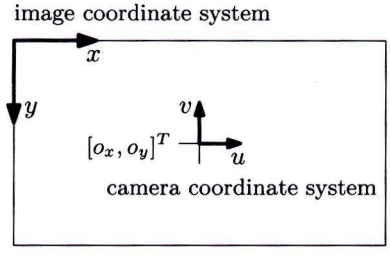

Fig. 2: Comparing the image $(x, y)^T$ and camera $(u, v)^T$ coordinate system.

point (o_x, o_y) are sensor specific parameters. One of the most suitable methods to obtain those parameters is to use the depth images that can be captured by the sensor, together with a transparent checkerboard, as shown in Figure 1.

Now, each voxel coordinate in the world coordinate system P_{world} can be transformed to each camera coordinate point P_{cam} by using the camera dependent extrinsic parameters, by

$$P_{cam} = RP_{world} + T. \tag{1}$$

Knowing the camera focal length and the principal point, the 3D camera coordinate point $P_{cam} = [X, Y, Z, 1]^T$ can be represented in a pixel position $(u, v)^T$ as shown in Figure 2. This can be calculated by use of the projection matrix, with $\lambda = Z$ as homogeneous scaling factor:

$$\lambda \begin{bmatrix} u \\ v \\ 1 \end{bmatrix} = \begin{bmatrix} f & 0 & o_x & 0 \\ 0 & f & -o_y & 0 \\ 0 & 0 & 1 & 0 \end{bmatrix} \begin{bmatrix} X \\ Y \\ Z \\ 1 \end{bmatrix}. \tag{2}$$

Finally, after verifying each voxel for all sensors, the free space model is reconstructed. The reliability of the reconstruction is increased by combining the information from multiple sensors. If a sensor

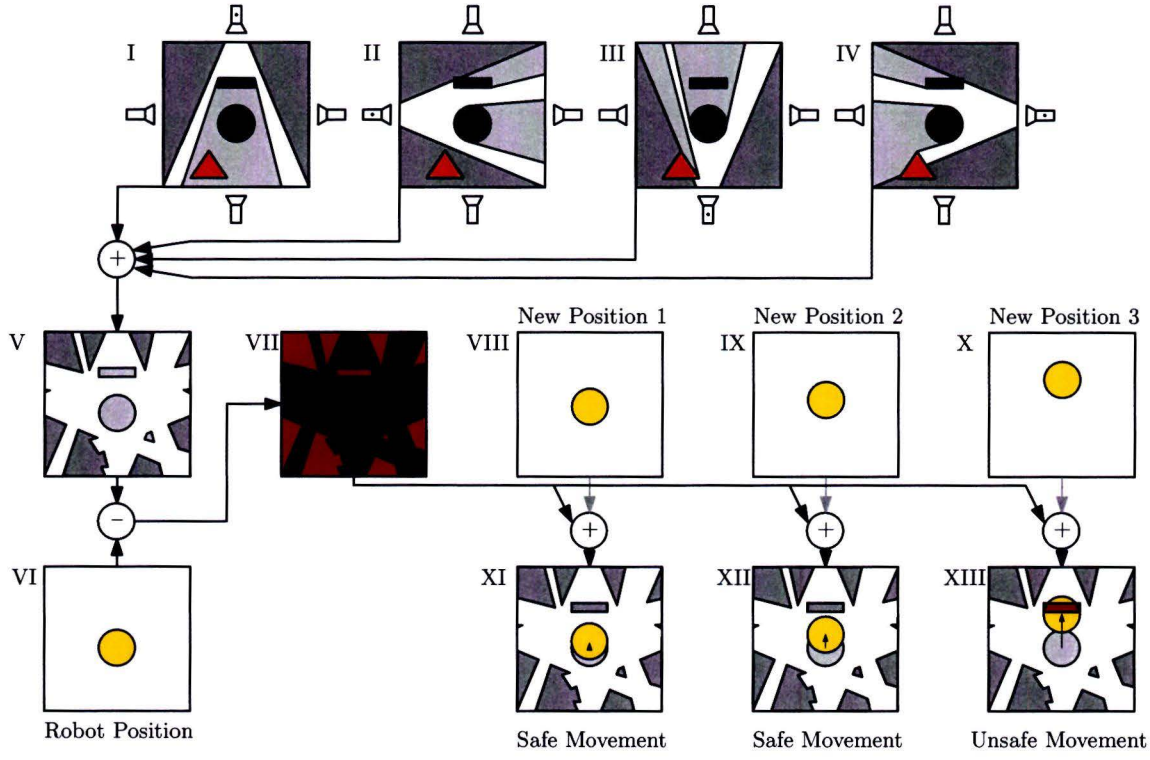

Fig. 3: Graphical overview of the reconstruction algorithm. Using the depth images (I-IV) a Free Space reconstruction (V) can be made. By subtracting the current known Robot position (VI) the movement area (green) of the robot can be reconstructed in (VII). By projecting the new positions (VIII-X) in (VII), the collision detection algorithm can be used to detect safe (XI-XII) and unsafe (XIII) moving distances.

detects a voxel as the edge or surface of an object, three or more sensors are needed to overrule this.

In Figure 3, a $2D$ graphical overview of the algorithm to reconstruct the free space is given. For each of the obtained images (I-IV), the free space detected by each of the sensors is converted to the real world coordinates by use of the extrinsic parameters R and T. By combining all this free space information into a single model (V), a representation of the free space is given. Because the robot cannot collide with itself, the known robot position (VI) can be added to (V) as free space, which finally results in the free space model (VII). Now, for the collision detection, model (VII) can be used to test if the area is free for the intended movements (XI-XIII).

By correlating the data of multiple sensors, the robot will get more movement freedom as shown in (V) and (VII) than a non-correlated system. This is because for a single sensor it is only possible to guarantee safety for a movement perpendicular towards the sensor, where correlated sensors can provide information in more directions than the number of sensors. Another advantage of correlating the data from multiple sensors is that the accuracy of the reconstruction is increased by fusion of sensor data, which makes it possible to eliminate measurement errors.

3.3 Number of Cameras

Because occlusions can occur for setups with multiple objects and where it is assumed that the number and orientation of objects in the environment are not known, it is impossible to find a camera layout wherein all points in the volume can be seen continuously.

Therefore, the requirement is set that for a complete empty model, each volume point has to be seen by at least 3 sensors which are all at least 100 degrees separated from each other in the horizontal plane. This requirement for the sensors is chosen because for a voxel to get occluded in all 3 sensors, there should be 3 objects present each blocking another line of sight, which is assumed to be not highly probable.

By using the captured images of the volume without any objects present, for each individual volume point the number and angle of views can be tested. First, a number of cameras is distributed

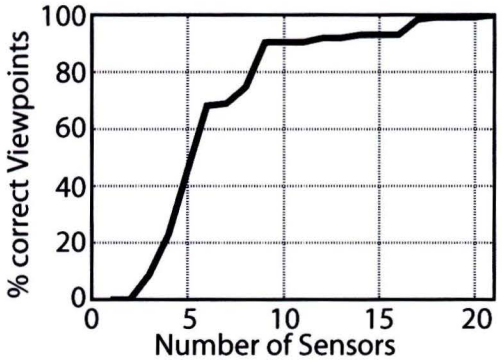

Fig. 4: Percentage of valid points for the empty setup depending on the number of sensors.

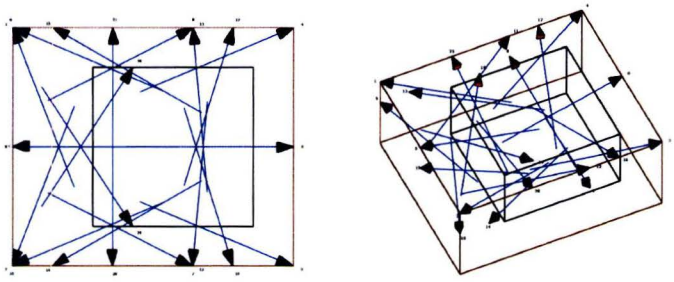

(a) Top View. (b) 3D View.

Fig. 5: Overview of Camera placement with sight of line views and interesting area.

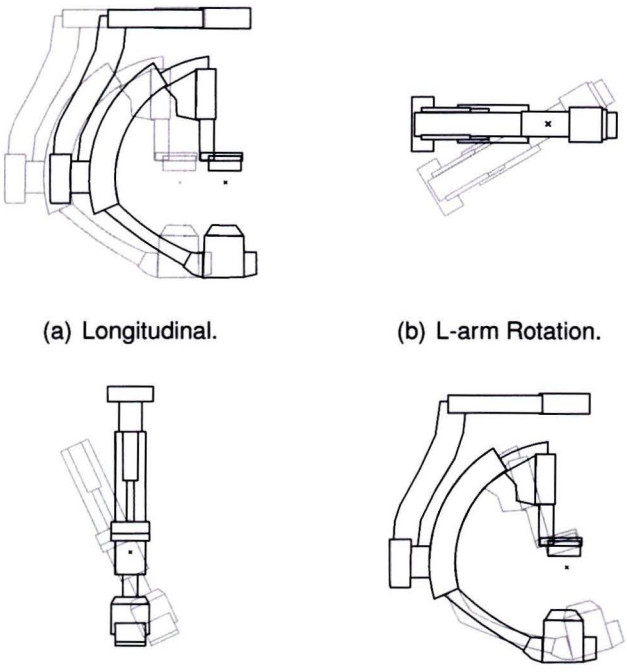

(a) Longitudinal. (b) L-arm Rotation.

(c) Propeller Rotation. (d) C-arc Rotation.

Fig. 6: The four movement directions of a C-arc.

evenly along the sides of the room. By validating each voxel for each set of sensors, the layout and/or number of sensors in the setup can be adjusted iteratively until the requirements are met. The iterative process of validation is shown in Figure 4. This finally results in a setup with a total number of 21 sensors, as shown in Figure 5.

4 Collision Avoidance

To avoid any collisions between the controlled C-arc and its environment, the free space model from Section 3 is used. Furthermore, the $3D$ model of the C-arc, together with its current and intended position and orientation are used. By using this data, a collision avoidance algorithm can be designed.

4.1 Algorithm

For detecting collisions, the free space model is used as starting point. By using the model of the robot together with its current position and orientation, the volume points that are occupied by the C-arc can be eliminated. By eliminating those points, the collision detection can verify new positions without taking the old position into account. Now, intended movement positions of the C-arc, as shown in Figure 6, can be projected into the volume.

For each of the moving directions of the C-arc the maximum speeds and braking times are known. By using this information, three distances can be calculated. The minimum distance S is the breaking distance if the C-arc is moving at full speed. The medium distance M is twice the distance of the shortest distance, where the largest distance L is five times the shortest distance.

If any object is detected within the minimum distance, the C-arc movement will be stopped directly to prevent the collision. The medium distance is used to start decelerating the movements to prevent any upcoming possible collision more smoothly, where the largest distance can be used to provide the controller of the C-arc the information that the C-arc is approaching an object.

5 Simulations and Experiments

Before the actual system will be implemented, a simulation model is used for verification of the accuracy and to test the collision avoidance, where

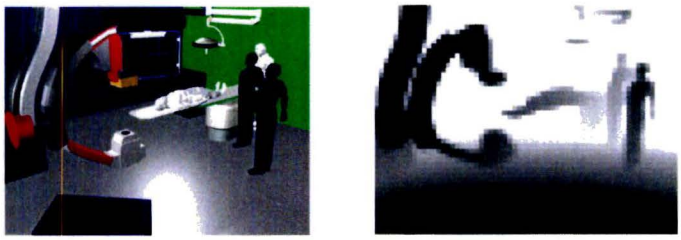

(a) Colour. (b) Depth.

Fig. 7: Colour and Depth image of the Simulated Scene in Blender.

a scale model is used to show a real world implementation. In the simulation environment, Time-of-Flight sensors [15]–[18] are simulated to generate the depth images, where Microsoft Kinects™ [19] are used in the scale model.

The Time-of-Flight sensors are used for the actual scene because of the measurement accuracy at larger distances. The Kinects, which provide depth information by laser triangulation [19] are chosen for the scale model. Because of the depth sensing method of the Kinect, they are only suitable for distances shorter then $4[m]$. This makes them perfectly suitable for the scale model, but not for the actual system with distances up to $7[m]$.

Because it is possible to export the simulated setup as voxel model, the software is extremely useful to get quantitative results of the reconstruction accuracy by comparing the simulation with the reconstruction. An example of the simulated setup and a depth image are given in Figure 7.

The first measure to verify the reconstruction is the reconstruction accuracy where the occupancy of each voxel the reconstruction is compared to occupancy in the simulation model.

The second measure for verification is by implementing the collision avoidance in both the reconstruction and the simulation model and comparing the output of both, which makes it possible to conclude if the reconstruction is safe or not.

The scale model is used to test the calibration and correlation of the cameras. The scale model is built on a 1:5 scale model available at Philips Healthcare and uses four Microsoft Kinects™.

5.1 Simulation

With the simulated setups as shown in Figure 11 in Appendix A, the algorithms as discussed in the previous sections are verified.

5.1.1 Reconstruction Accuracy

To define how accurate a reconstruction of the setup is made, the reconstruction achieved by combining the depth image data is compared to the volumetric simulated model of the setup. For each voxel it can be determined whether or not it is free or occupied for both the reconstruction and simulation model. To analyse the results, there are four cases wherein each voxel can be quantified as shown in Table 1.

TABLE 1: Cases for Reconstruction.

Case	Simulation Model	Reconstruction	Voxel Verdict
1	Free	Free	Correct Free
2	Free	Occupied	Incorrect Free
3	Occupied	Occupied	Correct Object
4	Occupied	Free	Incorrect Object

Cases 1 and 3 from Table 1 are situations where the reconstruction is exactly the same as the simulation model. For Case 2, free space in the simulation model is detected as an object in the reconstruction. The main reason for this problem is occlusion of this point for all viewpoints. This leads to undesirable behaviour because the C-arc will be stopped moving while it is not necessary. Fortunately, no collisions will occur either. For Case 4, where an actual object is not detected, the collision avoidance will not be able to prevent collisions with this object. A possible reason for not detecting objects is when these are smaller than the detectable object size by the sensors.

To test the reconstruction accuracy, six different setups are build in the simulation environment. These setups are some of the most common positions and orientations of the C-arc in an intervention room, together with a standard set of objects present in the room. An overview of the setups is given in Appendix A.

5.1.2 Collision Avoidance

Starting with the same six setups as used for the reconstructions, several future movements of the C-arc are tested in the reconstructed and simulated model. The intended movements and setups are shown in Figure 12 in Appendix B. By comparing the results between the reconstruction and simulation model, it can be concluded whether the reconstruction is safe s, slightly too safe ts, much too safe tts or unsafe u.

5.2 Scale Model

To verify if the reconstruction also works in reality, a $1:5$ scale model of an intervention room is used.

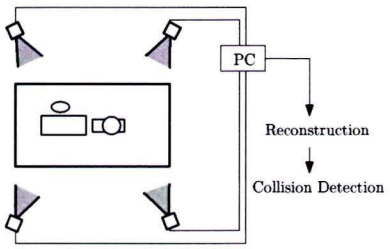

Fig. 8: Hardware layout for the scale model setup.

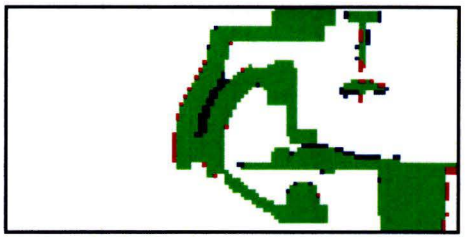

Fig. 9: Graphical output of the reconstruction algorithm, with the cases 1 (white), 2 (blue), 3(green) and 4 (red).

As depth sensors, Microsoft Kinects™ are used.

Because only four Kinects are used in this setup, as shown in Figure 8, some areas might get occluded for large number of objects. Therefore, the number of objects is restricted to the C-arc, a patient table and a doctor.

6 Results

For the simulated and scale model setup, the reconstruction and collision avoidance algorithm are tested, which results are presented in this section.

6.1 Simulations

6.1.1 Reconstruction Accuracy

To analyse the reconstructions, the free and occupied volumes from ground truth models from the simulation are compared with the reconstructed free space grid.

In Table 2 an overview of the reconstruction accuracy is given, where the percentages of Cases 1 and 3 from Table 1 are shown. A graphical representation of the reconstruction accuracy is given in Figure 9.

As can be concluded from Table 2, the free spaces in the setups are reconstructed with an average accuracy of 98.9% where the objects are reconstructed with an accuracy of 91.1%. This implies that 1.1% of the free space is seen as object, where 8.9% of the objects are defined as free space.

TABLE 2: Results Reconstruction.

Setup	Free [%]	Occupied [%]
1	99.1	89.1
2	98.7	94.0
3	98.7	93.0
4	98.6	89.0
5	99.2	90.2
6	99.0	87.3

The reconstruction accuracy of the Free space can be concluded as sufficient, because a certain rate of occlusions can be expected.

The reduced object reconstruction accuracy of 91.1% can be explained because some of the present objects are detected slightly smaller than they actually are. This is because of the quantisation of the volume. Another reason for this reduction in accuracy is that some of the present objects are smaller than $0.10[m]$. Because of the field-of-view of the simulated camera and the number of pixels in the sensor, only objects larger than $0.10[m]$ are detectable. With newer versions of Time-of-Flight cameras with higher resolution, this problem will be over.

6.1.2 Calibration errors

For a real setup, it is assumed that the sensors are calibrated perfectly. Unfortunately, this will not be the case for all situations. To verify the robustness in alignment, it is tested what the effects of miss alignment are on the accuracy of the reconstruction.

As a first test, the angles of the rotation matrices R for all cameras are disturbed by a random noise up to $\pm 1[^\circ]$, which corresponds to a miss alignment of approximately 1 pixel. Validating the reconstruction for those miss alignments, the reconstruction accuracy did not change.

The translation matrices T are disturbed with a random noise up to $\pm 1[cm]$ as a second test. Again, the reconstruction shows the same accuracy as without disturbance.

The robustness of the reconstruction accuracy can be attributed to the merging of sensor information and the coarse discretisation of the volume.

6.1.3 Collision Avoidance

For the analysis of the collision avoidance, future positions of the C-arc are tested in the setups. After testing all the movements, the output of the collision avoidance algorithm for Setup 6 are given in Table 3. By comparing the results between the reconstruction and simulation, the safety of the

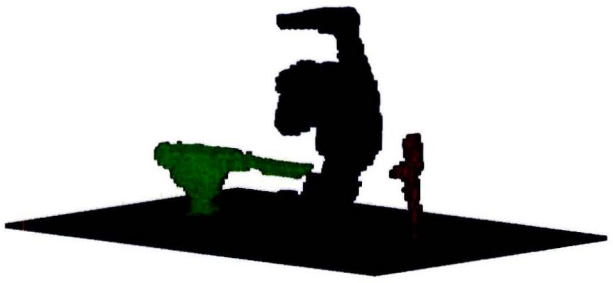

Fig. 10: Reconstruction Scale Model with the C-arc (blue), table (green) and a nurse (red).

reconstruction can be defined. According to the quantisation problem, only objects of $0.10[cm]$ and larger are detectable. To show the shortcomings of the reconstruction, 2 collision avoidance tests are executed with objects smaller than $0.10[cm]$, where it is expected that those tests should give an unsafe verdict.

TABLE 3: Results Collision Detection Setup 6.

Movement	Reconstruction	Simulation	Verdict
Carc Rotation	M	L	ts
2× Carc Rotation	S	S	s

The results for the other collision detection setups are given in Appendix C. As can be seen, 27 out of 35 Reconstruction provide the correct collision detection verdict, where 6 out of 35 verdicts are safer than necessary. Only 2 out of the 35 reconstructions provide a verdict that is not safe and where an collision can occur, which is exactly as expected.

For the verdicts where the reconstruction is too safe, the volume between the C-arc and the colliding object is occluded from all viewpoints which makes it impossible to see it. This can be dealt with by implementing an override function which allows the operator to move the C-arc at low speeds in those areas.

6.2 Scale Model Results

With the obtained depth information from each of the four depth sensors and the calibration data, a reconstruction of the scene is generated. This results in a reconstruction as shown in Figure 10.

After implementation of the collision avoidance setup, the maximum free moving distances can be calculated. These distances have a maximum deviation of $\pm 5[mm]$, which corresponds to a deviation of $\pm 25[mm]$ in a real size system. This is smaller than the quantisation in the real size simulation and therefore accurate enough.

7 Conclusion

In this paper a new approach for collision avoidance in an unknown $3D$ dynamic robotic environment was introduced. The main contribution is a general applicable safety system that is reliable, all collisions that should be detected are detected, for environments containing multiple unknown objects.

By use of the robotic model a collision detection and avoidance algorithm are implemented, tested and verified, both in simulations as well as on a scale model. The results show that the system is safe and reliable, because all of the collisions that should be detected are detected.

Besides safe navigation, the reconstruction can be used for other purposes such as path planning, object tracking or gesture recognitioning.

The main advantage of this system over other safety systems is that it does not need any a priori information about the scene or present objects to operate, except for the model of the machine itself.

The reconstruction algorithm can work with an arbitrary number of sensors, wherein it is possible to implement free space information from other sensors as well.

Further research can be addressed to optimal positioning of the cameras. An optimal positioning can reduce the number of sensors and therefore the costs. By taking the time aspect into account, temporal filtering and dynamic object tracking are possible add-ons to increase the accuracy of the reconstruction and collision avoidance.

APPENDIX A
SIMULATION SETUPS

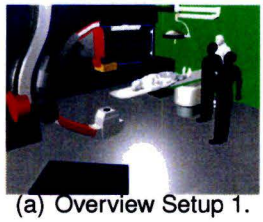

(a) Overview Setup 1.

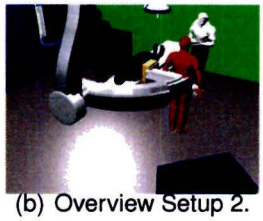

(b) Overview Setup 2.

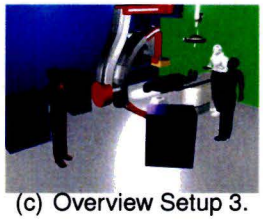

(c) Overview Setup 3.

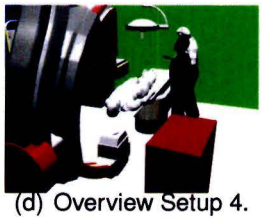

(d) Overview Setup 4.

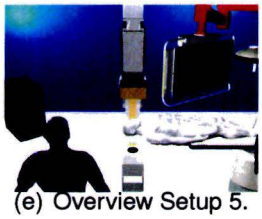

(e) Overview Setup 5.

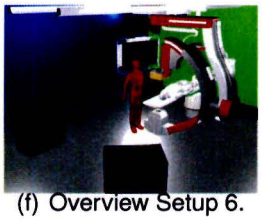

(f) Overview Setup 6.

Fig. 11: Overviews of the different setups.

APPENDIX B
COLLISION DETECTION SETUPS

In this appendix, the intended movements of the C-arc in the six setups as shown in Appendix A are shown. Single arrows show translations, where double arrows show rotation.

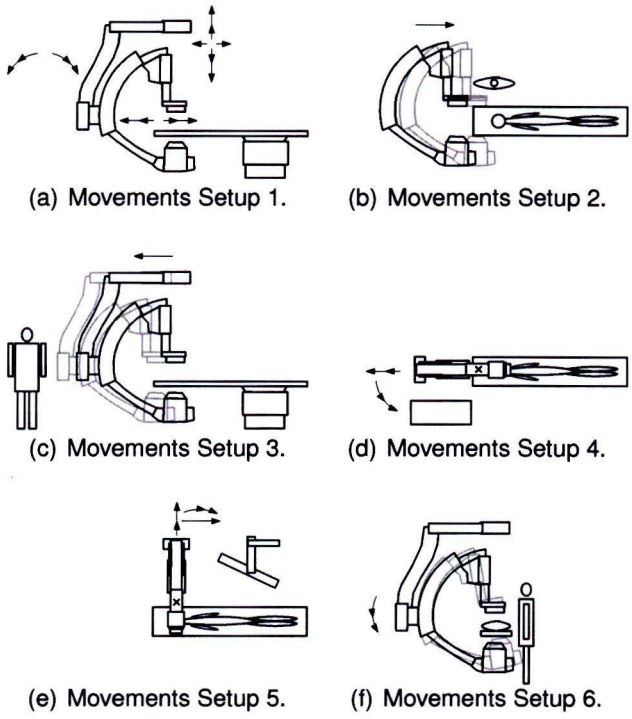

(a) Movements Setup 1. (b) Movements Setup 2.

(c) Movements Setup 3. (d) Movements Setup 4.

(e) Movements Setup 5. (f) Movements Setup 6.

Fig. 12: Movements for each setup.

APPENDIX C
COLLISION DETECTION RESULTS

The shortest distance S is the maximum breaking distance if the C-arc is moving at full speed. The medium distance M is twice the minimum distance, where the largest distance L is five times the minimum distance. 0 implies that no collision is detected for all three distances.

By comparing the results between the reconstruction and simulation, it can be concluded whether the reconstruction is safe s, slightly too safe ts, much too safe tts or unsafe u.

TABLE 4: Results Collision Avoidance for all Setups with movements as indicated in Appendix B.

Movement	Reconstruction	Simulation	Verdict
Setup 1			
Larm +	0	0	s
Larm -	L	L	s
Propeller +	0	0	s
Propeller -	0	0	s
Carc +	0	0	s
Carc -	0	0	s
Long +	0	0	s
Long -	0	0	s
Setup 2			
Long	M	L	ts
2 × Long	M	L	ts
3 × Long	M	M	s
4 × Long	L	L	s
Setup 3			
Long	0	0	s
2 × Long	L	L	s
3 × Long	L	L	s
4 × Long	M	M	s
5 × Long	S	S	s
Setup 4			
Prop	M	0	ts
2 × Prop	S	0	tts
3 × Prop	S	S	s
Larm	L	L	s
2 × Larm	L	L	s
3 × Larm	M	M	s
4 × Larm	S	S	s
Setup 5			
Long	L	L	s
2 × Long	L	L	s
3 × Long	M	M	s
Prop	L	L	s
Long - Prop	M	L	u
2 × Long - Prop	S	M	u
Larm	L	L	s
Long - Larm	L	M	ts
2 × Long - Larm	M	M	s
Setup 6			
Carc Rotation	M	L	ts
2× Carc Rotation	S	S	s

REFERENCES

[1] D. Henrich and T. Gecks, *Multi-Camera Collision Detection Between Known and Unknown Objects*, in Distributed Smart Cameras, 2008, pp. 1, 2008.

[2] Z. Wu, N.I. Hristov, T.L.Hedrick, T.H. Kunz, M. Betke, *Tracking a Large Number of Objects from Multiple Views*, in Conference on Computer Vision, 2009.

[3] L. Balan and G.M. Bone, *Real-time 3D Collision Avoidance Method for Safe Human and Robot Coexistence*, in IEEE International Conference on Intelligent Robots and Systems, 2006, pp. 276-282, Beijing, China.

[4] C. Wang and F. Wang, *A Knowledge-based Strategy for Object Recognition and Reconstruction*, in IEEE International Conference on Information Technology and Computer Science, 2009.

[5] I. Masaaki, K. Yoshinari and M. Michihiko, *4 π Measurement System: A Complete Volume Reconstruction System for Freely-moving Objects*, Multisensor Fusion and Integration for Intelligent Systems, 2003, pp. 119-224, 2003.

[6] F. Brisc, *Multi-resolution Volumetric Reconstruction Using Labeled Regions*, in Image Analysis and Interpretation, 2004, pp. 114, 2004.

[7] Y. Ding, J. Yu, P. Sturm, *Multiperspective Stereo Matching and Volumetric Reconstruction*, in IEEE 12th International Conference on Computer Vision, 2009, pp. 1827-1834, 2009.

[8] C. Zach, M. Sormann, K. Karner, *High-Performance Multi-View Reconstruction*, in IEEE 3rd Int ernational Symposium on 3D Data Processing, Visualisation and Transmission, 2006.

[9] B. Winkler, *Safe Space Sharing Human-Robot Cooperation Using a 3D Time-of-Flight Camera*, International Robots and Vision Show, 2007.

[10] S. Bouyagoub, D.R. Bull, N. Canagarajah and A. Nix, *Automatic Multi-Camera Placement and Optimisation Using Ray Tracing*, in IEEE 17th International Conference on Image Processing, 2010, pp. 681-684, 2010.

[11] E. Hörster and R. Lienhart, *Approximating Optimal Visual Placement*, in IEEE ICME 2006, pp. 1257-1260, 2006.

[12] J. O'Rourke, *Art Gallery Theorems and Algorithms*, Oxford University Press, New York, 1987.

[13] S. Fuchs and G. Hirzinger, *Extrinsic and depth calibration of ToF-cameras*, in Computer Vision and Pattern Recognition, 2008, pp. 1-6, June 2008.

[14] Y. Morvan, *Acquisition, Compression and Rendering of Depth and Texture for Multi-View Video*, PhD dissertation, Chapter 2.2, ISBN 978-90-386-1682-7, 2009.

[15] M. Lindner and A. Kolb, *Lateral and Depth Calibration of PMD-Distance Sensors*, Advances in Visual Computing, Computer Graphics Group, University of Siegen, Germany.

[16] A. Kolb, E. Barth and R. Koch, *ToF-Sensors: New Dimensions for Realism and Interactivity*, in IEEE Computer Vision and Pattern Recognition Workshops, 2008, pp. 1-6, 2008.

[17] R.Z. Whyte, A.D. Payne, A.A. Dorrington and M.J. Cree, *Multiple range imaging camera operation with minimal performance impact*, Proc. SPIE-IS&T Electronic Imaging, SPIE vol. 7538, pp. 75380I, 2010.

[18] *PMD [vision] S3 Datasheet V. No. 20090601*, available online: http://www.pmdtec.com/fileadmin/pmdtec/downloads/documentation/datasheet_s3.pdf, June 2010

[19] A. Shpunt, *Depth Mapping Using Multi-Beam Illumination*, United States Patent Application Publication, Pub. No. US 2010/0020078 A1, Jan. 28, 2010.

[20] Blender, June 2010 [online]. Available: http://www.blender.org.
[21] K.S. Booth, D.R. Forseyand A.W. Paeth, *Hardware Assistance for Z-Buffer Visible Surface Algorithms*, Computer Graphics and Applications, IEEE, vol 6.11, pp. 31-39, nov 1986.